19th Australasian Fluid Mechanics Conference
Melbourne, Australia
8-11 December 2014

An Investigation of Evaporation from Single Saline Water Droplets: Experimental and Theoretical Approaches

M. H. Sadafi[1], I. Jahn[1], A. B. Stilgoe[2] and K. Hooman[1]

[1]School of Mechanical and Mining Engineering

The University of Queensland, QLD 4072, Australia

[2]School of Mathematics and Physics

The University of Queensland, QLD 4072, Australia

Abstract

Heat transfer to and mass transfer from NaCl-water droplets are investigated both numerically and experimentally. A new model is presented and used to simulate saline water droplet evaporation. The model is robust enough to be applied for various initial concentrations and conditions of the droplet, ambient conditions, and dissolved media properties. The model is validated using experimental data obtained in this study on top of those already available in the literature. The experimental apparatus as well as the processing routines to optically measure droplet evaporation at a range of ambient conditions are presented. Data were collected for droplets with an initial radius of 500 µm at three temperatures 25 ^oC, 35 ^oC, and 45 ^oC and three air velocities 0.5 m/s, 1.5 m/s, and 2.5 m/s to provide a comprehensive validation dataset. Based on experimental and simulation data, a correlation is presented that captures the start time of solid formation. This time plays an important role in cooling tower design as it shows the time that the outer surface of the droplet dries. Using the validated model, it is shown that for 500 µm radius droplets with 5% initial mass concentration the start time of reaching the final size is 24.9% less than evaporation time of a pure water droplet. Also, the net energy required to evaporate the droplet falls by 12.2%compared to a pure water droplet. Using saline water in spray-cooling has two major effects: the energy extracted from the air per unit droplet volume is reduced (which can be compensated for by increasing the liquid flow rate). Moreover, compared to the time taken for the evaporation of a pure water droplet, the period with wet surface is shorter as a result of crust formation around the saline water droplet. This allows a shorter distance between spray nozzles and heat exchangers.

Introduction

Improving the efficiency of dry cooling towers has always been a challenge for designers. For instance, in arid areas production capacity losses of about 50% are predicted [1]. To enhance the performance of dry cooling towers, hybrid methods are suggested to decrease inlet air temperature. Two hybrid methods are available in dry cooling systems: evaporative spray cooling of the inlet air, and using water deluge to cool the air. Spray assisted dry cooling towers are more efficient and cost effective in arid areas as they do not require a large volume of water. In liquid spray cooling systems small droplets increase the contact area with the air resulting in higher total heat and mass transfer. Applying spray cooling in dry areas, however, faces an obvious challenge of fresh water scarcity. However, as an alternative, saline water might be available in spray-assisted dry cooling towers (hybrid). For example, in arid areas in Queensland, Australia a large volume of water is produced in the production of natural gas from coal-bed methane. Methane desorbs from coal if pressure is decreased in the underground reservoir by water pumping [2]. Therefore, saline water will be available as a valuable source for spray cooling systems. There are, nonetheless, some dissolved and insoluble materials in this water. Kinnon et al. showed that NaCl is the main salt in the saline water from coal-bed methane production [3]. According to those authors, NaCl constitutes about 84% (mass based) of the total dissolved salt in Bowen Basin in Queensland. Due to similarities between the physical properties of NaCl and the other dissolved salts, NaCl may be considered as the main dissolved salt in saline water.

To simulate the evaporation process from solid-containing droplet, researchers have suggested two [4, 5] and three-stage models [6-9]. In general, the evaporation of droplets can be described as follows (see “figure 1”):

1. The droplet is warmed/cooled to be close to ambient conditions,
2. Evaporation takes place during an isothermal phase,
3. First particles form at the bottom of the droplet [10] and grow to cover the upper part,
4. The remaining water is then evaporated followed by complete drying.

The slow formation of the crust is considered in the mathematical modelling by Sadafi et al. [11]. In their four-stage model they showed that the droplets shrink even after presence of solid particles on the surface which results in a better agreement with the experimental results compared to former models [11].
Using microscope digital camera, Sadafi et al. monitored the droplet size at low air velocities to note that the droplets shrink after crust formation in slow evaporation under standard room conditions [11].

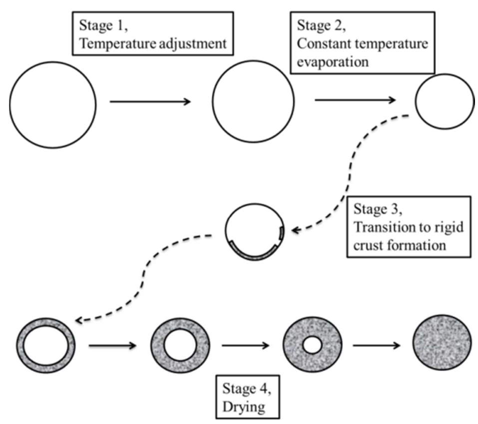

Figure 1. Stage of evaporation of a solid containing water droplet

Theoretical Modelling

The four-stage model developed by Sadafi et al. [11] was used in this study.

Four-Stage Model

According to this model, during the first stage of evaporation, the temperature of a saline water droplet adjusts to approach the wet-bulb temperature. Evaporation in this stage is negligible compared to the later stages. Next, the second stage starts and the droplet size decreases. This stage is an approximately isothermal process with a nearly constant evaporation rate. As water evaporation continues, solid concentration rises to the critical concentration which, in turn, depends on the solid properties. Once the critical concentration is reached, the third stage kicks off and solid crystals are formed in the lower part of the droplet. Then, they start to extend up to the droplet sides as the third stage progresses.

Finally, the fourth stage starts once a solid crust forms around the entire droplet. This solid crust then grows in thickness until all the liquid is evaporated. This crust is assumed to be a porous medium allowing the diffusion of water vapour through its pores.

Assuming axisymmetric shape for the droplet, homogenous properties, and neglecting directional forces (e.g. gravity) [12], the energy equation for the droplet is [9]:

$$\frac{\partial(\rho c_p T)}{\partial t} = \frac{1}{r^2}\frac{\partial}{\partial r}\left(kr^2\frac{\partial T}{\partial r}\right) \tag{1}$$

where T is the temperature (of the droplet in the first and second stages or of the crust or wet-core during the fourth stage). The following boundary conditions are applied for the first and second stage:

$$\begin{cases} \dfrac{\partial T}{\partial r} = 0, & r = 0 \\ h\left(T_g - T\right) = k_d\dfrac{\partial T}{\partial r} + h_{fg}\dfrac{\dot{m}_v}{A_d}, & r = R_d \end{cases} \tag{2}$$

where R_d is the droplet outer radius in the first and second stage. The following conditions apply for the fourth stage:

$$\begin{cases} \dfrac{\partial T_{wc}}{\partial r} = 0, & r = 0 \\ k_{cr}\dfrac{\partial T_{cr}}{\partial r} = k_{wc}\dfrac{\partial T_{wc}}{\partial r} + h_{fg}\dfrac{\dot{m}_v}{A_d}, & r = R(t) \\ T_{wc} = T_{cr}, & r = R(t) \\ h\left(T_g - T_{cr}\right) = k_{cr}\dfrac{\partial T_{cr}}{\partial r}, & r = R_{cr} \end{cases} \tag{3}$$

where R(t) is the radius of the interface between the wet-core and the crust.

As latent heat is dominant, compared to sensible heat, the energy balance equation applied to the first and second stages and the wet-core in the fourth stage can be simplified to [9]:

$$h_{fg}\dot{m}_v = h(T_g - T)A_d \tag{4}$$

Changes in the droplet radius in the first two stages and the wet-core radius in the fourth stage is determined by solving "equation (5)" [9]. To calculate the wet-core radius in the fourth stage, the effective surface area in the right hand side of "equation (5)" must be adjusted to include the porosity:

$$\frac{d(r)}{dt} = -\frac{1}{4\rho\pi r^2}\dot{m}_v \tag{5}$$

The vapour mass flow rate from the wet-core in the fourth stage is obtained using "equation (6)" as described in [11]:

$$\dot{m}_v = -\frac{p_g}{\mathcal{R}\left(T_{cr,s} + T_{wc,s}\right)}M_w D_{v,cr}\frac{8\pi\varepsilon^\beta\left(R_p r_{wc}\right)}{\left(R_p - r_{wc}\right)} \ln\left[\frac{p_g - p_{v,i}}{p_g - \left(\dfrac{\mathcal{R}}{4\pi M_w h_D R_p^2}\dot{m}_v + \dfrac{p_{v,\infty}}{T_g}\right)T_{cr,s}}\right] \tag{6}$$

Here, it is assumed that the vapour diffuses through a number of Stefan tubes. The argument in the logarithmic term shows the vapour mass concentration gradient through the pore. The multiplier is the density of the vapour times the vapour diffusion coefficient and the pore cross-sectional area.

To calculate the heat and mass transfer coefficients at the gas-liquid interface when gas is forced to flow over (and around) the droplet, the correlations from Ranz and Marshall [12] are used:

$$Nu = 2 + 0.6Re_d^{\frac{1}{2}}Pr^{\frac{1}{3}} \tag{7}$$

$$Sh = 2 + 0.6Re_d^{\frac{1}{2}}Sc^{\frac{1}{3}} \tag{8}$$

In the model developed by Sadafi et al. [11], the third stage is introduced by a adding a weighting factor "z" to blend the equations of evaporation and drying (second and fourth) stages. Here, z is the volume fraction of the wet volume to the whole particle. It is equal to unity at the beginning of the third stage and goes to zero at the end of this period. Details of the calculation of droplet properties in different stages are presented in [11].

A Lagrangian formulation of the flow field is used to solve the governing equations for the first and second stages. A grid with 64 cells in the radial direction is implemented and a fixed time step of 0.1 s is used for the transient implicit solution. For the fourth stage, a uniform grid distribution with size of 4 µm in the radial direction is implemented and an adaptive time step with initial value of 0.05 s is used to obtain the transient implicit solution. Results obtained using shorter (half) time steps and spatially-refined grids are found to be within 1% of those obtained from the baseline. The obtained results from the model are validated in [11].

Experimental Study

In this section, the experimental results for water droplets containing NaCl are presented and compared with those from theoretical model.

Experimental Setup

A variable speed fan is used to provide a wide range of air velocities. Before passing through an aluminium flow straightener, the air stream is heated using a heater. The heater resistive wires are automatically controlled using a feedback loop to achieve a prescribed temperature as measured by the two thermocouples (to measures dry-bulb and wet-bulb temperatures). The droplet is suspended in the channel using a filament and its size is continuously measured by a microscope digital camera as described in [11].

As the evaporation progresses (especially after solid formation) the photo capture may be inaccurate because the droplet loses its axisymmetric shape. This is because the camera only captures one view of the droplet outline at a time. Therefore, in the case of a concave or convex shape on the droplet surface, the actual size is missed by the camera. To overcome this issue a computer controlled low speed (less than 5 rpm) servo motor is used to rotate the filament and the droplet during the experiment. This ensures that the pictures of the droplet can be taken from different angels.

Test Conditions

Since the objective of this research is to study the evaporation behaviour of droplet solution in dry cooling towers, relevant conditions are chosen for experimental tests. A typical dry cooling tower in Queensland operates at around 45oC on hot summer days. However, this temperature can be less than 25°C in some periods of a year. Therefore, three temperatures of 25, 35, and 45 °C are selected for the ambient air temperature. To study the influence of air flow rate on convection heat transfer three air speeds of 0.5, 1.5, and 2.5 m/s were chosen to simulate typical air velocities inside cooling towers. As NaCl is reported to be the main solid in the saline water [3]; NaCl solutions with initial mass concentration of 5% was chosen. A range of relative humidity values were chosen as it varies throughout the year. A micropipette with the accuracy of 0.01 µL was used to generate droplets with initial diameters of about 1 mm.

Data Collection/Processing

Droplet diameter was continuously monitored and recorded using an optical microscope and video camera to measure the changes in the droplet size during the experiment. Using the servo motor allows estimating a more accurate size for the droplet by averaging images taking at different angels. The minimum and maximum frequency of the servo motor is 0.1 Hz and 1 Hz, respectively, whilst the photos are captured at 0.055 Hz. The uncertainty of radius measurements is less than 2.2% with servo speeds of 0, 3, and 6 rpm (using the procedure recommended by Moffat [13]). Each experimental test was repeated at least three times. The results fell within the respective uncertainty bounds, thereby demonstrating that our laboratory studies are repeatable with a high level of reliability. Following the procedure recommended by Moffat [13], the uncertainty in measuring the droplet size is found to be less than 3.68%.

Experimental Results

"Figure 2" to "figure 4" show the predicted as well as the experimentally-measured radius of the droplet when the air temperature is set at 25 °C. Note that the predicted final sizes of the droplets are 269 µm, 259 µm, and 267 µm for 0.5, 1.5, and 2.5 m/s air velocity, respectively.

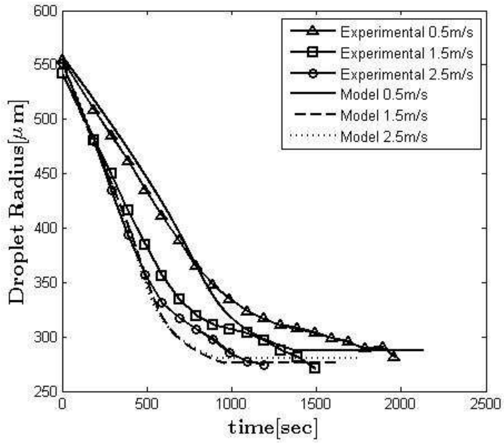

Figure 2. Radius of the droplet for 25 °C

"Figure 3" shows the experimental data and simulated results for 35 °C gas temperature at different air stream velocities. The predicted final sizes are in a good agreement with the experimental results.

As shown in "figure 4" the predicted final solid sizes for different air velocities in 45 °C perfectly correspond to those measured in the experimental tests. Moreover, as the air velocity increases the agreement between the model prediction and experimental data improves.

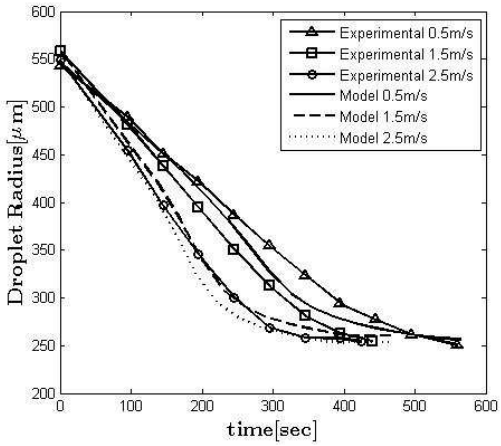

Figure 3. Radius of the droplet for 35 °C

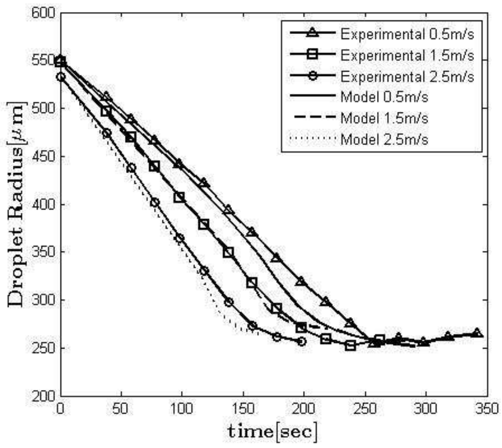

Figure 4. Radius of the droplet for 45 °C

Discussion

From a design analysis point of view, predicting the start time of solid formation (beginning of the fourth stage) is the most important factor. This time, $t_{4th\ stage}$, is the time needed for the droplet to reach its final size and the complete dry out of the droplet surface. As such, it is an important parameter to monitor in order to avoid corrosion of the heat exchanger surfaces and particle deposition.

Applying dimensionless analysis, a proper combination of the parameters will make all the recorded data to collapse on a single line as shown in "figure 5". In this figure the start time of solid formation (beginning of the fourth stage) is plotted against the variable f. The data show that $t_{4th\ stage}$ is a linear function of f and can be expressed as follows:

$$t_{4th\ stage} = 2.3599 \times 10^{11} . \frac{m_0 R_0^{0.4}}{k_g^{0.4}(T_g - T_{wb}) h^{0.6} c_0^{0.2}} \qquad (9)$$

In this equation the initial radius, mass, and concentration in addition to the dry bulb and wet-bulb temperatures, gas conductivity, and the convection heat transfer coefficient are grouped. The heat transfer coefficient is a function of Nusselt, Prandtl, and Reynolds numbers which incorporates the influence of air velocity in the above correlation. Also, the influence of relative humidity is taken into consideration through the $(T_g - T_{wb})$ term.

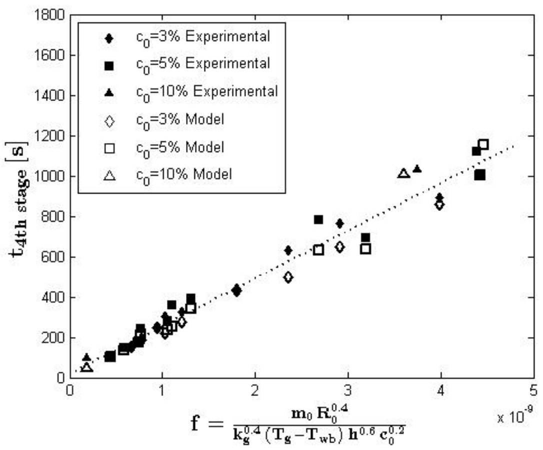

Figure 5. Presented correlation to determine solid formation time

In addition to the experimental and model results, additional experimental tests for 3% and 10% initial concentrations and different temperatures were performed to show the generality of "equation (9)" in "figure 5". The lowest measured $t_{4th\ stage}$ had 10% initial concentration, 2.25 m/s air velocity, and 83.5 ^oC air temperature. The initial radius of the droplet for this test is 520 μm. The experimental value of $t_{4th\ stage}$ is 49 s whilst the model predicts 44.9 s.

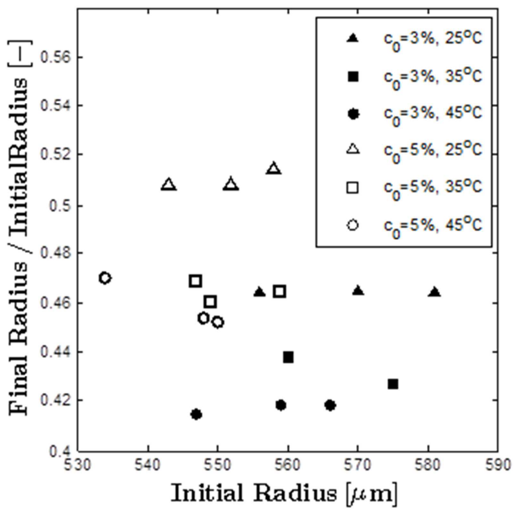

Figure 6. Fraction of the final radius to initial radius of the droplet (MATLAB results)

"Figure 5", demonstrates that "equation (9)" is a very reliable prediction of $t_{4th\ stage}$ especially for higher air temperatures, velocities, and initial concentrations. The R2 value for the correlation is 0.9684 and the maximum error is 6.26% which is related to 5% initial concentration, 35 ^oC, and 1.5 m/s air velocity. The experimental results show a better agreement with predicted values for smaller droplet sizes and lower wet-bulb temperatures (lower relative humidity).

"Figure 6" shows the fraction of the final solid radius to the initial radius of the droplet. Due to higher volume of NaCl for 5% initial concentration, the final size of the solid particle is proportionally larger than that observed for 3%. As shown in this figure, the gas temperature affects the final size as the crystal in slower evaporation forms with more porosity. Therefore, the final size of the dried solid in 25 ^oC in larger than 35 ^oC, and they both are larger than 45 ^oC gas temperature for the same initial concentration.

Conclusions

A robust mathematical model was presented that can be applied for a wide range of initial and boundary conditions to predict the behaviour of evaporation of saline water droplets. This model was validated with a comprehensive set of experimental tests. These tests were performed for different air velocities, gas temperature and initial concentrations. Based on the experimental data and model a correlation, relating the time of crust formation to droplet and ambient conditions was created. Observations from the study are that replacing pure water by saline water in cooling systems has two important effects: lower heat capacity of the cooling water, and shorter time with wet surface. The first effect can be compensated by using a larger volume of water whilst the second effect allows a decrease of the distance between the nozzle and heat exchanger. As the current work focuses on droplets in isolation, further work is needed to study the behaviour of droplets in spray cooling systems. Specifically the total displacement, corrosion levels and deposition of solid particles need to be investigated.

References

[1] Ashwood A & Bharathan D. *Hybrid cooling systems for low-temperature geothermal power production*. Golden, CO: National Renewable Energy Laboratory; 2011. p. 1-62.

[2] Rice CA & Nuccio V. *Water Produced with Coal-Bed Methane*. USGS Fact Sheet FS-156-002000.

[3] Kinnon ECP, Golding SD, Boreham CJ, Baublys KA & Esterle JS. Stable isotope and water quality analysis of coal bed methane production waters and gases from the Bowen Basin, Australia. *International Journal of Coal Geology*. 2010;82:219-31.

[4] Abuaf N & Staub FW. *Drying of Liquid-solid Slurry Droplets: General Electric,* Corporate Research and Development; 1985.

[5] Elperin T & Krasovitov B. Evaporation of liquid droplets containing small solid particles. *International Journal of Heat and Mass Transfer*. 1995;38:2259-67.

[6] Nešić S & Vodnik J. Kinetics of droplet evaporation. *Chemical Engineering Science*. 1991;46:527-37.

[7] Farid M. A new approach to modelling of single droplet drying. *Chemical Engineering Science*. 2003;58:2985-93.

[8] Dalmaz N, Ozbelge HO, Eraslan AN & Uludag Y. Heat and Mass Transfer Mechanisms in Drying of a Suspension Droplet: A New Computational Model. *Drying Technology*. 2007;25:391-400.

[9] Mezhericher M, Levy A & Borde I. Theoretical Drying Model of Single Droplets Containing Insoluble or Dissolved Solids. *Drying Technology*. 2007;25:1025-32.

[10] Charlesworth DH & Marshall WR. Evaporation from drops containing dissolved solids. *AIChE Journal*. 1960;6:9-23.

[11] Sadafi MH, Jahn I, Stilgoe AB & Hooman K. Theoretical and experimental studies on a solid containing water droplet. *International Journal of Heat and Mass Transfer*. 2014;78:25-33.

[12] Ranz WE & Marshall WR. Evaporation from Drops. *Chemical Engineering Progress*. 1952;48:141-6.

[13] Moffat RJ. Describing the uncertainties in experimental results. *Experimental thermal and fluid science*. 1988;1:3-17.